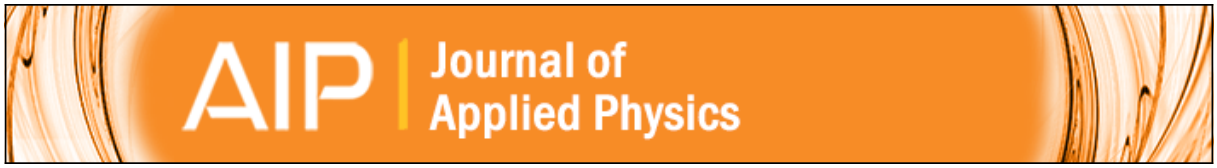

Multi-mode noise analysis of cantilevers for scanning probe microscopy

M. V. Salapaka, H. S. Bergh, J. Lai, A. Majumdar, and E. McFarland

Citation: Journal of Applied Physics **81**, 2480 (1997); doi: 10.1063/1.363955

View online: http://dx.doi.org/10.1063/1.363955

View Table of Contents: http://scitation.aip.org/content/aip/journal/jap/81/6?ver=pdfcov

Published by the AIP Publishing

Multi-mode noise analysis of cantilevers for scanning probe microscopy

M. V. Salapaka
Department of Mechanical and Environmental Engineering, University of California at Santa Barbara, Santa Barbara, California 93106

H. S. Bergh
Department of Chemical Engineering, University of California at Santa Barbara, Santa Barbara, California 93106

J. Lai
Department of Mechanical and Environmental Engineering, University of California at Santa Barbara, Santa Barbara, California 93106

A. Majumdar
Department of Mechanical Engineering, University of California, Berkeley, California 94720

E. McFarland[a)]
Department of Mechanical and Environmental Engineering, University of California at Santa Barbara, Santa Barbara, California 93106

(Received 30 August 1996; accepted for publication 22 November 1996)

A multi-mode analysis of micro-cantilever dynamics is presented. We derive the power spectral density of the cantilever displacement due to a thermal noise source and predict the cantilevers's fundamental resonant frequency and higher harmonics. The first mode in the multi-mode model is equivalent to the traditional single-mode model. Experimental results obtained with a silicon nitride cantilever at 300 K are in excellent qualitative agreement with the multi-mode model. The multi-mode model may be used to obtain accurate values of the cantilever properties such as the elastic modulus, effective mass, thickness and moment of inertia. © *1997 American Institute of Physics.* [S0021-8979(97)04105-4]

I. INTRODUCTION

Micro-cantilevers are widely used for the detection of forces in a variety of scanning force microscopes.[1] Atomic interaction forces, magnetic forces, and electric forces have been monitored using the deflection of the micro-cantilever as a measure of the forces.[1] The cantilever deflection is typically measured by optical or by electrical means.

Although extrinsic factors such as background vibration, room temperature fluctuations, and transient interactions between the cantilever and the surrounding gaseous medium frequently limit the force detection in practice, fundamentally it is the thermal noise of the cantilever that limits the sensitivity of scanning force microscopes. An in-depth understanding of the noise sources and their power spectra in micro-cantilevers is lacking. However, it may be useful in improving cantilever design and for the analysis of experimental data. Previous thermal noise estimates were based on an analysis where the cantilever is modeled as a single spring-mass-damper system.[1] Estimates of the thermal noise amplitude in a free undamped cantilever considering all modes of vibration of the cantilever were recently obtained.[2] However, this does not provide information on the vibrational amplitude in a frequency range, which is useful for lock-in detection schemes.

The estimates of the power spectral density of the cantilever displacement is of particular interest for studies of extremely weak forces such as detected in magnetic force microscopy. It was proposed by Sidles and co-workers[3–6] that magnetic resonance imaging with single spin sensitivity is possible using detection techniques which employ a micro-cantilever. The basic experimental principles were demonstrated by Rugar and co-workers who detected a net spin of approximately 10^8 electrons and a net spin of approximately 10^{12} protons.[6,7] The limiting factor on sensitivity of these detection schemes is thought to be the thermal noise.[7]

In Section II of this paper, we give a multi-mode analysis of the dynamics of a damped cantilever which is subjected to time-varying forces. In Section III, the power spectral density of the cantilever deflection due to the thermal source is derived based on a multi-mode model of the cantilever. Section IV establishes the relationship of the traditional model to the multi-mode model. In Section V, we present experimental methods and in Section VI we give results and discussion. Finally, we give the summary in Section VII.

II. MULTI-MODE MODEL OF THE CANTILEVER

Traditionally, micro-cantilevers for force microscopy have been modeled as a single spring-mass-damper system.[1] It was suggested that in certain scanning schemes subharmonics of the fundamental modes of the cantilever are driven. To predict these subharmonics it is essential that a multi-mode model of the cantilever be used.[8] Better estimates of the thermal noise effects on the cantilever displacement and the error involved in using a single-mode approximation can be obtained by using the multi-mode model. With this motivation, we give a detailed multi-mode analysis of the cantilever dynamics below.

[a)]Electronic mail: mcfar@engineering.ucsb.edu

 0021-8979/97/81(6)/2480/8/$10.00

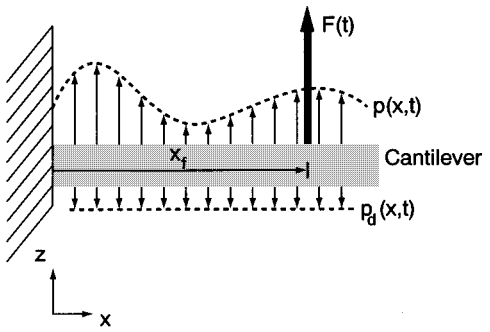

FIG. 1. A schematic showing a cantilever subjected to an applied load, $p(x,t)$, the damping force, $p_d(x,t)$ assumed constant per unit length and a concentrated force, $F(t)$, applied at a distance x_f from the base of the cantilever.

Figure 1 shows a cantilever subject to multiple loading. One end of the cantilever is fixed and the other end is free. The distributed applied load per unit length is given by $p(x,t)$. A concentrated load $F(t)$ is applied at a distance x_f from the base of the cantilever. The distributed load may be due to a piezoelectric material on the cantilever and the concentrated force may be due to the interaction between the sample and the cantilever tip. The damping force per unit length is denoted by $p_d(x,t)$. The length of the cantilever is L, its Young's modulus of elasticity is E, its cross sectional area is A, and its area moment of inertia is I (all in SI units).

A. Undamped free vibration

In the absence of damping and applied loads, the equation of motion of the cantilever is given by

$$EI\frac{\partial^4 z(x,t)}{\partial x^4}+\rho A\frac{\partial^2 z(x,t)}{\partial t^2}=0,$$

$$z(x,0)=a(x),\quad \frac{\partial z(x,0)}{\partial t}=b(x), \tag{2.1}$$

where $a(x)$, $b(x)$ are the initial conditions of the cantilever and $z(x,t)$ is the displacement of the cantilever. We will use the convention that $f'(x,t)$ denotes the spatial derivative, $\partial f(x,t)/\partial x$ and $\dot{f}(x,t)$ denotes the time derivative, $\partial f(x,t)/\partial t$. It can be shown[2] that the solution of Eq. (2.1) has the form

$$z(x,t)=\sum_{j=1}^{\infty} C_j \sin(\omega_j t+\delta_j)\phi_j, \tag{2.2}$$

with

$$\phi_j(x)=(\sin\lambda_j L+\sinh\lambda_j L)(\cos\lambda_j x-\cosh\lambda_j x)+(\cos\lambda_j L+\cosh\lambda_j L)(\sinh\lambda_j x-\sin\lambda_j x), \tag{2.3}$$

where λ_j is a solution of

$$\cos\lambda_j L\cosh\lambda_j L+1=0. \tag{2.4}$$

The j^{th} mode deformation of the cantilever is given by $\phi_j(x)$, whereas the wavelength of the j^{th} mode is given by $\lambda_j L$. The wavelengths are arranged in an ascending order ($\lambda_1<\lambda_2<\ldots$). The relation between the wavelength and frequency of mode j is given by

$$(\lambda_j L)^4=\frac{\omega_j^2\rho A L^4}{EI}. \tag{2.5}$$

It can be shown that the cantilever deformations ϕ_j satisfy the relations:

$$\int_0^L \phi_j(x)\phi_k(x)dx=\delta_{kj}LI_j, \tag{2.6}$$

$$\int_0^L \phi_j''(x)\phi_k''(x)dx=\delta_{kj}\lambda_j^4 LI_j, \tag{2.7}$$

$$\int_0^L \phi_j(x)dx=-\frac{2(\cos\lambda_j L+\cosh\lambda_j L)}{\lambda_j}=:J_j, \tag{2.8}$$

$$\phi_j(L)=2(\cos\lambda_j L\sinh\lambda_j L-2\sin\lambda_j L\cosh\lambda_j L), \tag{2.9}$$

$$\phi_j'(L)=-2\lambda_j(\sinh\lambda_j L\sin\lambda_j L), \tag{2.10}$$

where $I_j=(\sin\lambda_j L+\sinh\lambda_j L)^2$, $\delta_{kj}=0$ if $k\neq j$ and $\delta_{kj}=1$ if $k=j$. Conveniently, $\omega_j^2=k_j/m_j$ if we define

$$k_j:=EI\int_0^L \phi_j''(x)\phi_j''(x)dx$$

and

$$m_j:=\rho A\int_0^L \phi_j(x)\phi_j(x)dx. \tag{2.11}$$

Table I gives the values of important parameters for the first five modes.

B. Forced vibration with damping

To study the dynamics of the cantilever subjected to time varying forces we apply the *principle of virtual work* to obtain the equation of motion.[9] Let the displacement of the cantilever at position x and time t be given by $z(x,t)$. Suppose the cantilever is given a virtual displacement of $\delta u(x,t)$. The elastic work and the inertial work done by the cantilever are given by[9]

$$-EI\int_0^L z''(\delta u)''dx \quad\text{and}\quad -\rho A\int_0^L \ddot{z}(x,t)\delta u(x,t),$$

respectively, whereas the work done by the external applied forces and the damping force are given by

$$\int_0^L p(x,t)\delta u(x,t)dx+F\delta u(x_f,t)$$

and

$$-\int_0^L p_d(x,t)\delta u(x,t)dx,$$

respectively. Using the principle of virtual work whereby the net work must be zero, we obtain

$$\int_0^L\{-EIz''(\delta u)''-\rho A\ddot{z}(x,t)\delta u(x,t)-p_d(x,t)\delta u(x,t)+p(x,t)\delta u(x,t)\}dx+F\delta u(x_f,t)=0. \tag{2.12}$$

TABLE I. Important parameters for the first five modes.

$\lambda_j L$	1.875	4.694	7.855	10.996	14.137
$\cos(\lambda_j L)$	-0.300	-0.0184	-0.001	4.257×10^{-4}	1.669×10^{-4}
$\cosh(\lambda_j L)$	3.3371	54.6493	1.2893×10^{3}	2.9818×10^{4}	6.8959×10^{5}
$\sin(\lambda_j L)$	0.9541	$-.99998$	1	-1	1
$\sinh(\lambda_j L)$	3.1837	54.6402	1.2893×10^{3}	2.9818×10^{4}	6.8959×10^{5}
$\phi_j(L)$	-8.27	107.27	-2.738×10^{3}	5.996×10^{4}	-1.379×10^{6}
I_j	17.1215	2.877×10^{3}	1.6649×10^{6}	8.89×10^{7}	4.735×10^{11}
J_j/L	-3.2401	-23.2769	-328.2742	-5.42×10^{3}	-9.755×10^{4}
$\frac{m_j}{\rho AL}$	17.1215	2.877×10^{3}	1.6649×10^{6}	8.89×10^{7}	4.735×10^{11}
$\frac{k_j L^3}{EI}$	211.615	1.3969×10^{6}	6.3382×10^{9}	1.299×10^{13}	1.899×10^{16}
$\frac{c_j}{\xi L}$	17.1215	2.877×10^{3}	1.6649×10^{6}	8.89×10^{7}	4.735×10^{11}
$\omega_j^2\frac{\rho AL^4}{EI}$	12.3596	485.4811	3.807×10^{3}	1.462×10^{4}	3.9942×10^{4}

We assume that the damping is uniform and given by $p_d(x,t)=\xi\dot{z}(x,t)$. It can be shown that any function $r(x)$ which satisfies the boundary conditions imposed by the fixed-free cantilever defined between 0 and L can be expanded as $r(x)=\Sigma_{k=1}^{\infty}\phi_k(x)q_k$ where $\phi_k(x)$ were obtained from the free undamped vibration.[9] Thus, any deformation of the cantilever can be represented as a weighted combination of the fundamental mode deformations of the unforced cantilever. Therefore coefficients $q_k(t)$ and $\delta u_k(t)$ exist such that

$$z(x,t)=\sum_{k=1}^{\infty}\phi_k(x)q_k(t)$$

and

$$\delta u(x,t)=\sum_{k=1}^{\infty}\phi_k(x)\,\delta u_k(t). \tag{2.13}$$

Substituting Eq. (2.13) into Eq. (2.12), we obtain

$$\sum_{j=1}^{\infty}\sum_{k=1}^{\infty}EI\int_0^L\phi_k''\phi_j''dx q_k(t)\,\delta u_j(t)+\sum_{j=1}^{\infty}\sum_{k=1}^{\infty}\rho A\int_0^L\phi_k\phi_j dx\ddot{q}_k(t)\,\delta u_j(t)+\sum_{j=1}^{\infty}\sum_{k=1}^{\infty}\xi\int_0^L\phi_k\phi_j dx\dot{q}_k(t)\,\delta u_j(t)$$

$$=\sum_{j=1}^{\infty}\int_0^L p(x,t)\phi_j(x)dx\,\delta u_j(t)+\sum_{j=1}^{\infty}F(t)\phi_j(x_f)\,\delta u_j(t).$$

Therefore,

$$\sum_{j=1}^{\infty}\left(EI\int_0^L[\phi_j''(x)]^2dx q_j(t)+\rho A\int_0^L\phi_j^2(x)dx\ddot{q}_j+\xi\phi_j^2(x)dx\dot{q}_j-p_j(t)-F_j(t)\right)\delta u_j(t)=0,$$

where

$$p_j(t):=\int_0^L p(x,t)\phi_j(x)dx$$

and

$$F_j(t):=\phi_j(x_f)F(t).$$

As $\delta u_j(t)$ is arbitrary, we have

$$m_j\ddot{q}_j(t)+c_j\dot{q}_j(t)+k_jq_j(t)=p_j(t)+F_j(t)\quad\text{for all } j=1,2,\ldots, \tag{2.14}$$

where the jth modal mass, spring constant, and damping coefficient are defined as

$$m_j:=\rho A\int_0^L\phi_j^2(x)dx,\quad k_j:=EI\int_0^L(\phi_j''(x))^2$$

and

$$c_j:=\xi\int_0^L\phi_j^2(x)dx.$$

To obtain the necessary initial conditions of $q_j(t)$ for Eq. (2.14), we assume that

$$z(x,0)=a(x)\quad\text{and}\quad\dot{z}(x,0)=b(x).$$

From Eq. (2.13), we have

$$a(x)=\sum_{k=1}^{\infty}\phi_k(x)q_k(0)\quad\text{and}\quad b(x)=\sum_{k=1}^{\infty}\phi_k(x)\dot{q}_k(0).$$

Multiplying the above equations by $\phi_j(x)$ and integrating, we have the necessary conditions

$$q_j(0)=\frac{\rho A\int_0^L a(x)\phi_j(x)dx}{m_j}$$

and

$$\dot{q}_j(0)=\frac{EI\int_0^L b(x)\phi_j(x)dx}{k_j}. \tag{2.15}$$

If the initial conditions are zero [that is $a(x)=b(x)=0$] then $q_j(0)=\dot{q}_j(0)=0$. Assuming zero initial conditions and taking the Fourier transform of Eq. (2.14), we obtain

$$z(x,\omega)=\sum_{j=1}^{\infty}\frac{p_j(\omega)+F_j(\omega)}{-m_j\omega^2+ic_j\omega+k_j}\phi_j(x). \tag{2.16}$$

Thus, we have obtained an expression of the cantilever displacement in terms of the forces on the cantilever.

III. THERMAL NOISE

Thermal noise is often the factor limiting the sensitivity of scanning probe microscopes. In this section the multimode model of the cantilever is used to obtain the effect of thermal noise on the cantilever displacement.

The potential energy in the beam at any time, t, is given by

$$PE(t)=\frac{1}{2}EI\int_0^L[z''(x,t)]^2dx. \tag{3.1}$$

Using Eq. (2.13), we have

$$PE(t)=\frac{1}{2}EI\sum_{l=1}^{\infty}\sum_{j=1}^{\infty}q_l(t)q_j(t)\int_0^L\phi_l''(x)\phi_j''(x)dx$$

$$=\frac{1}{2}\sum_{j=1}^{\infty}k_jq_j^2(t).$$

Note that $q_j(t)$ is the displacement of a simple harmonic oscillator of frequency $\omega_j=\sqrt{k_j/m_j}$. The expectation value for the energy of the quantized harmonic oscillator of frequency ω is simply[10]

$$\frac{\hbar\omega}{e^{\hbar\omega/k_BT}-1}. \tag{3.2}$$

That the expected value of the potential and kinetic energies are equal implies that the expected value of the potential energy of the j^{th} harmonic oscillator (which has frequency ω_j) is

$$\langle PE_j(t)\rangle=\frac{1}{2}\frac{\hbar\omega_j}{e^{\hbar\omega_j/k_BT}-1}, \tag{3.3}$$

where $\langle . \rangle$ denotes the expectation value and $PE_j(t):=\frac{1}{2}k_jq_j^2(t)$. For the first few modes which satisfy $\hbar\omega_j \ll k_BT$ we have $\langle PE_j(t)\rangle=\frac{1}{2}k_BT$. If we assume that the force on the cantilever is solely thermal in origin then the equation of motion for the j^{th} harmonic oscillator is given by

$$m_j\ddot{q}(t)+c_j\dot{q}(t)+k_jq_j(t)=p_j(t), \tag{3.4}$$

where $p_j(t)$ is the forcing due to thermal source. From Eq. (3.4), $q_j(t)$ can be considered to be the output of a linear time invariant system $H_j(\omega)$ for an input $p_j(t)$ and transfer function

$$H_j(\omega)=\frac{1}{-m_j\omega^2+ic_j\omega+k_j}. \tag{3.5}$$

Therefore the power spectral density of $q_j(t)$, $S_{q_jq_j}(\omega)$ is given by[11]

$$S_{q_jq_j}(\omega)=|H_j(\omega)|^2S_{p_jp_j}(\omega)$$

$$=\frac{1}{(k_j-m_j\omega^2)^2+c_j^2\omega^2}S_{p_jp_j}(\omega), \tag{3.6}$$

where $S_{p_jp_j}(\omega)$ is the power spectral density of $p_j(t)$. This implies that

$$\tfrac{1}{2}k_BT=\langle PE_j(t)\rangle=\tfrac{1}{2}k_j\langle q_j(t)^2\rangle=\tfrac{1}{2}k_jR_{q_jq_j}(0)$$

$$=\frac{1}{2}k_j\frac{1}{2\pi}\int_{-\infty}^{\infty}S_{q_jq_j}(\omega)d\omega$$

$$=\frac{1}{4\pi}k_j\int_{-\infty}^{\infty}\frac{1}{(k_j-m_j\omega^2)^2+c_j^2\omega^2}$$

$$\times S_{p_jp_j}(\omega)d\omega,$$

where $R_{q_jq_j}(\tau)$ is the autocorrelation function of $q_j(t)$ and is equal to $\langle q_j(t)q_j(t+\tau)\rangle$ [it is also the inverse Fourier transform of $S_{p_jp_j}(\omega)$]. Assuming p_j is white noise with a spectral density given by a constant σ_j^2, we have

$$\frac{1}{2}k_BT=\frac{\sigma_j^2}{4\pi}\int_{-\infty}^{\infty}\frac{k_j}{(k_j-m_j\omega^2)^2+c_j^2\omega^2}d\omega. \tag{3.7}$$

Assuming that the damping is small enough ($\xi^2<4EI\rho A\lambda_j^4$ for $j=1,\ldots N$), we can show that (see Appendix)

$$\int_{-\infty}^{\infty}\frac{1}{(k_j-m_j\omega^2)^2+c_j^2\omega^2}d\omega=\frac{\pi}{\omega_j^2c_jm_j}. \tag{3.8}$$

Therefore,

$$\sigma_j^2=2k_BTc_j. \tag{3.9}$$

Once the values of the σ_j^2 are evaluated from Eq. (3.9), we can obtain the power spectral density of the displacement of the cantilever due to thermal noise by the relation $z(x,t)=\Sigma_{j=1}^{N}q_j(t)\phi_j(x)$, where we have assumed that the effect of modes higher than N are negligible. As $q_j(t)$ are independent, it follows that

$$S_{zz}(\omega)=\sum_{j=1}^{N}S_{q_jq_j}(\omega)\phi_j^2(x). \tag{3.10}$$

Therefore, from Eq. (3.6), we have

$$S_{zz}(\omega)=\sum_{j=1}^{N}\frac{2k_BTc_j\phi_j^2(x)}{(k_j-m_j\omega^2)^2+c_j^2\omega^2}. \tag{3.11}$$

In many detection schemes, the measurement is restricted to frequencies well below ω_1. The root-mean-square displacement of the tip of the cantilever in a frequency range $[-\Delta\omega,\Delta\omega]$, is given by

$$\langle z^2(L)\rangle := \frac{1}{2\pi}\int_{-\Delta\omega}^{\Delta\omega} S_{zz}(\omega)\,d\omega$$

$$= \frac{1}{2\pi}\sum_{j=1}^{N} \int_{-\Delta\omega}^{\Delta\omega} \frac{2k_BTc_j\phi_j^2(L)}{(k_j-m_j\omega^2)^2+c_j^2\omega^2}\,d\omega. \tag{3.12}$$

If $\Delta\omega \ll \sqrt{k_1/m_1}=\omega_1$, then the following approximation holds

$$\langle z^2(L)\rangle = \frac{1}{2\pi}\sum_{j=1}^{N} \int_{-\Delta\omega}^{\Delta\omega} \frac{2k_BTc_j\phi_j^2(L)}{(k_j-m_j\omega^2)^2+c_j^2\omega^2}\,d\omega$$

$$\approx \sum_{j=1}^{N} \frac{4k_BTc_j\phi_j^2(L)\Delta\omega}{2\pi m_j^2\omega_j^4}. \tag{3.13}$$

This means that the root mean square displacement due to thermal noise in a frequency range $2\Delta f$ can be approximated as

$$\langle z^2(L)\rangle \approx \sum_{j=1}^{N} \frac{4k_BTc_j\phi_j^2(L)\Delta f}{m_j^2\omega_j^4}, \tag{3.14}$$

where $\Delta f=\Delta\omega/2\pi$.

It is to be noted that for the modes which satisfy $\hbar\omega_j \ll k_BT$ the total energy in the mode is a constant irrespective of the modal frequency. However, the energy in a certain range of frequencies depends on the transfer function $H_j(\omega)$ which in turn depends on the physical parameters of the cantilever. The design of the cantilever with respect to thermal noise issues is equivalent to shaping $H_j(\omega)$ for a desirable distribution of energy between different frequency ranges. It is desirable to shape $H_j(\omega)$ such that the energy due to thermal noise, in the frequency band in which the measurements are restricted, is minimized. $H_j(\omega)$ can be altered by changing the physical parameters of the cantilever. Another method which has not been widely exploited is to actively alter $H_j(\omega)$ using feedback control. Active control of the cantilever in scanning probe microscopes is studied (based on a one-mode model of the cantilever) in Refs. 12 and 13. The multi-mode model can be used to obtain a better model for active cantilever control.

IV. RELATION TO TRADITIONAL MODELS

Previous studies have modeled the cantilever as a single spring-mass system.[1] The damping is introduced to fit the experimental data. The spring constant is taken as $3EI/L^3$, and the effective mass is taken as $0.24\rho AL$ and are denoted by k and m, respectively.[1] Therefore, the equation of motion for the deflection of the tip, $z(t)$ of the cantilever is

$$0.24\rho AL\ddot{z}(t)+\frac{3EI}{L^3}z(t)=F(t), \tag{4.1}$$

where it is assumed that the only loading on the cantilever is the concentrated loading applied at the tip. Therefore $x_f=L$ and $p_d=p=0$. Note that if only one mode of the multi-mode model is used then

$$z(L,t)=\phi_1(L)q_1(t), \tag{4.2}$$

where $q_1(t)$ satisfies

$$m_1\ddot{q}_1(t)+k_1q(t)=F_1(t). \tag{4.3}$$

Multiplying the above equation by $\phi_1(L)$ and substituting $\phi_1(L)F(t)$ for $F_1(t)$, we have

$$m_1\ddot{z}(L,t)+k_1z(L,t)=\phi_1(L)^2F(t).$$

Substituting the values of m_1, k_1 and $\phi_1(L)$ from Table I, we obtain an equation identical to Eq. (4.1). This implies that the values of mass and spring constant as presented traditionally are related to m_1 and k_1 by

$$m=\frac{m_1}{\phi_1(L)^2} \quad \text{and} \quad k=\frac{k_1}{\phi_1(L)^2}. \tag{4.4}$$

In the single spring-mass-damper approximation, the damping effects are often described by the Q factor.[1] In the model presented here, we have used the parameter ξ to include damping effects. For the traditional single spring-mass-damper system, the equation of motion is given by

$$m\ddot{z}(t)+c\dot{z}(t)+kz(t)=f(t). \tag{4.5}$$

The predicted power spectral density of the Langevin forcing term, $f(t)$ is equal to $2k_BTc$.[1] The relation between Q factor and c is given by $Q=\sqrt{km}/c$. If only one mode of the multi-mode model is used then the equation of motion is given by

$$m_1\ddot{q}_1+c_1\dot{q}+kq=p_1(t), \tag{4.6}$$

where we have assumed that the only forcing is due to the thermal source $p_1(t)$. From the relation $z(L,t)=\phi_1(L)q_1(t)$ and Eq. (4.4), we know that the tip deflection dynamics are given by

$$m\ddot{z}(L,t)+\frac{c_1}{\phi_1^2(L)}\dot{z}(L,t)+kz(L,t)=\frac{p_1(t)}{\phi_1(L)}. \tag{4.7}$$

We can choose ξ such that $c=c_1/\phi_1^2(L)$. From Eq. (3.9) we can conclude that the power spectral density of $p(t)$ is given by $\sigma_1^2=2k_BTc_1$. This means that the forcing term in Eq. (4.7) has a power spectral density given by $\sigma_1^2[1/\phi_1^2(L)]=2k_BTc$. Thus for the choice of ξ above, the dynamics of the first mode of the multi-mode model we have presented agree with the dynamics of the traditionally employed model (note that some authors[6,14,15] employ a single-sided spectral density convention, rather than denote the double-sided convention used here resulting in a factor of 2 difference). Furthermore, the power spectral densities of the Langevin forcing term of the two models are identical. For

$$\frac{c_1}{\phi_1^2(L)}=c=\frac{\sqrt{km}}{Q}=\frac{1}{\phi_1^2(L)}\frac{\sqrt{k_1m_1}}{Q}, \tag{4.8}$$

we have

$$c_1=\frac{\sqrt{k_1m_1}}{Q}.$$

Substituting values from Table I, we have

$$\xi=\frac{3.515}{Q}\sqrt{\frac{EI\rho A}{L^4}}. \tag{4.9}$$

V. EXPERIMENTAL METHODS

The power spectral density of the cantilever tip displacement was measured experimentally. A diving-board cantile-

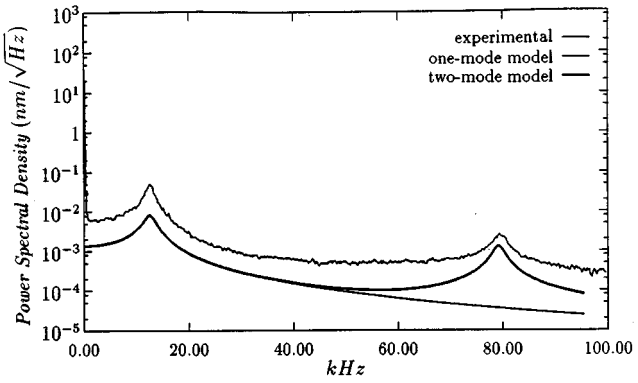

FIG. 2. The noise power spectral density of the detector output plotted against frequency. The plot predicted by the two-mode model agrees qualitatively with the experimental data. The experimental noise amplitude is greater than the predicted values is attributed to other noise sources. The traditional single-mode model agrees with the two-mode model for frequencies less than approximately 50 kHz.

ver (obtained from Digital Instruments) was used with a thickness of $0.42+/-0.03$ μm. The specified length L, breadth b and density ρ of the cantilever were 204 μm, 20 μm, and 3400 kg/m^3, respectively. The experiment was performed at a temperature, T, equal to 300 K. The cantilever was coated with Au/Cr which was removed by dipping the cantilever in the etchant solutions for Au and Cr, respectively.

The cantilever deflection was measured with an atomic force microscope (Nanoscope III AFM, Digital Instruments, CA) using a focused laser reflected from the cantilever onto a position-sensitive photodetector. The deflection of the cantilever was estimated by monitoring the position of the reflected laser. The signal from the photodetector was measured using the Hanning function of a dynamic signal analyzer (HP3562A).

The photodiode was calibrated from the slope of a force curve obtained from the interaction between the cantilever and a standard sample positioned on a calibrated piezoscanner of the atomic force microscope.[16] This allowed for the estimation of the cantilever deflection (in m/$\sqrt{\text{Hz}}$) from the output of the photodiode (in V/$\sqrt{\text{Hz}}$).

VI. RESULTS AND DISCUSSION

Figure 2 shows the power spectral density of the cantilever displacement as obtained by a one-mode model, by a two-mode model and by the experiment. The two-mode model is seen to predict the modal frequencies accurately.

It is likely that precise quantative agreement between the experimental data and the model is lacking due to errors in the cantilever parameters supplied by the manufacturer. The model can be used to accurately determine these physical parameters. As an example a range of values were specified for the thickness of the cantilever used in the experiment performed. However, for $t=0.43$ μm, the predicted and the experimental data showed good agreement suggesting that this might be the actual thickness of the cantilever. The actual displacement amplitude is greater than the predicted amplitude. We may attribute this to other noise sources such as the detector or the laser. However, none of the other noise sources are likely to excite the resonant modes of the cantilever and therefore the peaks in the plot are attributed to the thermal source.

We determined the value of c_1 by calculating ξ using the first mode [ξ was calculated using Eq. (4.9); the Q factor for the first mode was found to be 6] and then determining c_2 using the formula $c_2=\xi\int_0^L \phi_2^2(x)dx$. The plots in Figure 2 are based on these values. In the damping model, we assumed that the damping force is proportional to the velocity and is independent of the position along the cantilever. Because of these assumptions on the damping model, coefficients c_i are completely determined once ξ is fixed. To better identify the cantilever, one can abandon the assumptions on the damping (so that c_i can be fixed independently) made here and fix the values of c_i based on the experimental data.

The thermal noise calculations presented here are for a cantilever fixed at one end and free at another. However, in actual operation of scanning force microscopes this is not necessarily the operational configuration because the end with the tip is subjected to constraining forces. An analysis similar to the one carried out for the fixed-free cantilever can be performed when both ends of the cantilever are fixed by using the mode shapes of the unforced fixed-fixed cantilever to form the basis for the expansion of any possible deformation of the cantilever in the fixed-fixed configuration. The thermal noise in actual operation will lie between the values for fixed-free and the fixed-fixed cases.

The contribution of thermal noise to a particular measurement depends on the relevant frequency range. The area under the power spectral density curve for a specified frequency range is easily estimated and will represent the net contribution of the thermal noise to the measurement. Numerical values can be obtained using Equation (3.12).

The number of modes invoked in the multi-mode model depends on the specific frequency range of the experiment. If this range is far below the first cantilever harmonic then a single mode approximation is appropriate. Even if the measurements are restricted to the lower end of the frequency spectrum, the higher modes do contribute to the noise displacement. For data presented here (Figure 2), it is clear that if the measurements are restricted to a frequency range less than 40 kHz then the second mode can be neglected.

VII. SUMMARY

In this paper we have described the cantilever dynamics and thermal noise behavior of a cantilever relevant to scanning probe microscopy or other micro-cantilever based measurement techniques. Based on the free vibration modes of the cantilever, a detailed analysis of the dynamics of the forced cantilever is given. This analysis was used to predict the power spectral density of the cantilever deflection caused by thermal noise. The relationship to traditional noise analysis was established so that the results obtained here can be applied easily. The power spectral density of the displacement of a cantilever was obtained experimentally and compared to analytic predictions of the model. The results show good agreement. Fitting experimental data to the multi-mode model is shown to be a practical method for accurate identification of cantilever parameters.

ACKNOWLEDGMENTS

This research was supported by National Institute of Health (NIH) grant GM48887−04 to Professor Eric McFarland. Professor Arun Majumdar was supported by the National Science Foundation (NSF) through the NYI award CTS-9423141. We thank Mark Wendman from Digital Instruments for providing the cantilevers, Professor H. Weinberg for his helpful comments, and Pat White for help in preparing the manuscript.

APPENDIX

Evaluation of integrals and important parameters

Here, we give a closed form solution to the following integral

$$\int_{-\infty}^{\infty}\frac{1}{(k_j-m_j\omega^2)^2+c_j^2\omega^2}\,d\omega$$
$$=\frac{1}{m_j^2}\int_{-\infty}^{\infty}\frac{1}{(\omega_j^2-\omega^2)^2+\frac{c_j^2}{m_j^2}\omega^2}\,d\omega$$
$$=\frac{1}{m_j^2}\int_{-\infty}^{\infty}\frac{1}{\omega^4+\left(\frac{c_j^2}{m_j^2}-2\omega_j^2\right)\omega^2+\omega_j^4}\,d\omega,$$

where $\omega_j:=\sqrt{k_j/m_j}$. For notational convenience we define $b:=(c_j^2/m_j^2)-2\omega_j^2$ and evaluate the following integral:

$$\int_{-\infty}^{\infty}\frac{1}{\omega^4+b\omega^2+\omega_j^4}\,d\omega=\int_{-\infty}^{\infty}\frac{\frac{1}{\omega^2}}{\omega^2+b+\frac{\omega_j^4}{\omega^2}}\,d\omega=\frac{1}{\omega_j^2}\left(\int_0^{\infty}\frac{1+\frac{\omega_j^2}{\omega^2}}{\left(\omega-\frac{\omega_j^2}{\omega}\right)^2+2\omega_j^2+b}\,d\omega-\int_0^{\infty}\frac{1-\frac{\omega_j^2}{\omega^2}}{\left(\omega+\frac{\omega_j^2}{\omega}\right)^2-2\omega_j^2+b}\,d\omega\right).$$

We substitute $t=\omega-(\omega_j^2/\omega)$ and $\tau=\omega+(\omega_j^2/\omega)$ into the first and the second integrals, respectively, to obtain

$$\int_{-\infty}^{\infty}\frac{1}{\omega^4+b\omega^2+\omega_j^4}\,d\omega=\frac{1}{\omega_j^2}\left(\int_{-\infty}^{\infty}\frac{1}{t^2+b+2\omega_j^2}\,dt-\int_{-\infty}^{\infty}\frac{1}{\tau^2+b-2\omega_j^2}\,d\tau\right)$$
$$=\frac{1}{\omega_j^2}\left(\int_{-\infty}^{\infty}\frac{1}{t^2+\frac{c_j^2}{m_j^2}}\,dt-\int_{-\infty}^{\infty}\frac{1}{\tau^2+\frac{c_j^2}{m_j^2}-4\omega_j^2}\,d\tau\right).$$

Note that

$$\int_{-\infty}^{\infty}\frac{1}{t^2+\frac{c_j^2}{m_j^2}}\,dt=\frac{m_j}{c_j}\tan^{-1}\left(t\frac{m_j}{c_j}\right)\Bigg|_{-\infty}^{\infty}=\frac{m_j\pi}{c_j},$$

and

$$\int_{-\infty}^{\infty}\frac{1}{\tau^2+\frac{c_j^2}{m_j^2}-4\omega_j^2}\,d\tau=\frac{m_j\pi}{\sqrt{c_j^2-4\omega_j^2m_j^2}}\ \text{if}\ c_j^2-4\omega_j^2m_j^2>0=\frac{m_j}{2\sqrt{c_j^2-4\omega_j^2m_j^2}}\ \log\left(\frac{\tau-\frac{m_j}{\sqrt{c_j^2-4\omega_j^2m_j^2}}}{\tau+\frac{m_j}{\sqrt{c_j^2-4\omega_j^2m_j^2}}}\right)\Bigg|_{-\infty}^{\infty}$$
$$=0\ \text{if}\ c_j^2-4\omega_j^2m_j^2<0=0\ \text{if}\ c_j^2-4\omega_j^2m_j^2=0.$$

Also,

$$c_j^2-4\omega_j^2m_j^2=\xi\int_0^L\phi_j^2(x)dx-4k_jm_j=\left(\xi\int_0^L\phi_j^2(x)dx\right)^2-4EI\rho A\int_0^L\phi_j^2(x)dx\int_0^L[\phi_j''(x)]^2dx$$
$$=(\xi LI_j)^2-4EI\rho ALI_j\lambda_j^4LI_j=(LI_j)^2(\xi^2-4EI\rho A\lambda_j^4).$$

Therefore for $\xi^2<4EI\rho A\lambda_j^4$, we have

$$\int_{-\infty}^{\infty}\frac{1}{(k_j-m_j\omega^2)^2+c_j^2\omega^2}\,d\omega=\frac{1}{m_j^2}\frac{1}{\omega_j^2}\frac{m_j\pi}{c_j}=\frac{\pi}{\omega_j^2c_jm_j}.\tag{A1}$$

[1] Dror Sarid, *Scanning Force Microscopy* (Oxford University Press, New York, 1994).
[2] H. J. Butt and M. Jaschke, Nanotechnol. **6**, 17 (1995).
[3] J. A. Sidles, Appl. Phys. Lett. **58**, 2854 (1991).
[4] J. A. Sidles, Phys. Rev. Lett. **68**, 1124 (1992).
[5] J. A. Sidles, J. L. Garbini, and G. P. Drobny, Rev. Sci. Instrum. **63**, 3881 (1992).
[6] D. Rugar, C. S. Yannoni, and J. A. Sidles, Nature (London) **360**, 563 (1992).
[7] D. Rugar, O. Zuger, S. Hoen, C. S. Yannoni, H. M. Vieth, and R. D. Kendrick, Science **264**, (1994).
[8] N. A. Burnham, A. J. Kulik, G. Gremaud, and G. A. D. Briggs, Phys. Rev. Lett. **74**, 5092 (1995).
[9] R. R. Craig, *Structural Dynamics, An Introduction to Computer Methods* (Wiley, New York, 1981).
[10] R. P. Feynman, R. B. Leighton, and M. Sands, *The Feynman Lectures on Physics* (Addison-Wesley, Reading, MA, 1963).
[11] H. Stark and J. W. Woods, *Probability, Random Processes, and Estimation Theory for Engineers* (Prentice Hall, Englewood, NJ, 1994).
[12] J. L. Garbini, K. J. Bruland, W. M. Dougherty, and J. A. Sidles, J. Appl. Phys. **80**, 1951 (1996).
[13] K. J. Bruland, J. L. Garbini, W. M. Dougherty, and J. A. Sidles, J. Appl. Phys. **80**, 1959 (1996).
[14] U. Durig, O. Zuger, and A. Stadler, J. Appl. Phys. **72**, 1778 (1992).
[15] J. A. Sidles, J. L. Garbini, K. J. Bruland, D. Rugar, O. Zuger, S. Hoen, and C. S. Yannoni, Rev. Mod. Phys. **67**, 249 (1995).
[16] D. A. Walters, J. P. Cleveland, N. H. Thomson, P. K. Hansma, M. A. Wendman, G. Gurley, and V. Elings, Rev. Sci. Instrum. **67**, 3583 (1996).